AJBAR Vol. 4(6), December 2025: 81-96, ISSN: 2811-2881

Arid Zone Journal of Basic and Applied Research

Faculty of Science, Kashim Ibrahim University Maiduguri, Nigeria

Journal homepage: https://www.azjournalbar.com

Research Article

Nickel(II) and Copper(II) Complexes of Ampicillin-Based Schiff Base Ligands: Synthesis, Characterization, and Antimicrobial Evaluation

Matthew B. Mshelia, Mohammed B. Fugu, Ibrahim Waziri*, Grema A. Mala, Abubakar A. Ahmed, Ibrahim M. Wakil and Naomi P. Ndahi

Department of Pure and Applied Chemistry, University of Maiduguri, P.M.B. 1069, Maiduguri, Nigeria

***Corresponding author's Email**: waziriibrahim@unimaid.edu.ng, doi.org/10.55639/607.02010083

ARTICLE INFO:

Keywords:
Schiff base ligands,
Metal complexes,
Ampicillin derivatives,
Antimicrobial activity.

ABSTRACT

Two Schiff base ligands (HL1 and HL2) were synthesized through the condensation of ampicillin with 2-nitrobenzaldehyde and 2-hydroxy-1-naphthaldehyde, respectively, and subsequently complexed with Nickel(II) and Copper(II) ions to afford four new metal complexes (NiL1, CuL1, NiL2, and CuL2). The ligands and complexes were characterized using melting point determination, solubility tests, FTIR, UV–Visible spectroscopy, mass spectrometry, elemental analysis, and conductivity measurements. Spectroscopic data confirmed coordination through the azomethine nitrogen and the carbonyl oxygen of the amide group, with characteristic shifts in ν(C=N), ν(C=O), and ν(C–O) bands supporting tridentate chelation. Electronic spectra revealed ligand-cantered transitions for the free ligands and the appearance of d–d/LMCT bands in the metal complexes, suggesting octahedral coordination environments. The antimicrobial activities of the compounds were assessed against selected Gram-positive and Gram-negative bacteria (*S. aureus*, *S. pyogenes*, *E. coli*, *S. typhi*) and the fungal strain *C. albicans*. The complexes exhibited markedly higher activity than the free ligands, with CuL2 and NiL1 showing the broadest and most potent inhibition profiles. Structure–activity analysis indicates that increased π-conjugation (HL2-series) and the borderline Lewis acidity of Cu enhance biological potency. Overall, these results demonstrate the potential of ampicillin-derived Schiff base complexes as promising scaffolds for the development of new antimicrobial agents.

Corresponding author: Ibrahim Waziri **Email:** waziriibrahim@unimaid.edu.ng
Department of Pure and Applied Chemistry, University of Maiduguri, Nigeria

INTRODUCTION

Schiff bases and their metal complexes continue to attract considerable research attention due to their structural versatility, tunable donor properties, and wide range of biological and pharmaceutical applications (Malav & Ray, 2025; Shafie & Ashour, 2025). These compounds, typically formed through the condensation of primary amines with carbonyl compounds, possess an azomethine (–C=N–) functional group that plays a pivotal role in coordinating metal ions (Uddin *et al.*, 2025; Venkatesh *et al.*, 2024). The presence of additional donor sites such as –OH, –COOH, –NO_2, and aromatic rings further enhances their ability to form stable complexes with transition metals, thereby influencing their physicochemical and biological behaviour (Mushtaq *et al.*, 2024; Soroceanu & Bargan, 2022). Transition metal complexes of Schiff bases have been widely investigated for antimicrobial, anticancer, antioxidant, anti-inflammatory, and catalytic activities, owing to their ability to modulate the reactivity of the parent organic ligand through metal coordination (Krishna *et al.*, 2023; Kumar *et al.*, 2023).

Ampicillin, a β-lactam antibiotic of the penicillin class, is known for its broad-spectrum antimicrobial activity; however, the increasing rate of microbial resistance has limited its therapeutic efficiency (Bereda, 2022; Gambo *et al.*, 2023). Chemical modification of ampicillin through Schiff base formation has emerged as a promising strategy to enhance its pharmacological profile, improve stability, broaden antimicrobial activity, and overcome resistance mechanisms. Recent studies have demonstrated that derivatization of β-lactam antibiotics with aldehydes or aromatic substituents improve cell permeability, metal-binding capacity, and interaction with microbial targets (Al-Noor *et al.*, 2021; Arshi *et al.*, 2023; Subitha *et al.*, 2021). Yet, only limited reports exist on ampicillin-derived Schiff bases, and their transition metal complexes, particularly involving bioactive metal ions such as Nickel and Copper.

Given the biological importance of nickel(II) and copper(II) complexes, especially their known roles in enzyme mimicry, redox activity, and metal-assisted antimicrobial potency, investigating their coordination with ampicillin-based Schiff base ligands presents a valuable approach to developing novel antimicrobial agents (Lee & Lo, 2024; Sankar & Sharmila, 2023; Zavaroni *et al.*, 2025). Metal coordination often enhances lipophilicity, membrane penetration, and binding affinity of Schiff base ligands toward microbial biomolecules, thereby improving antimicrobial effectiveness through synergistic metal–ligand interactions (Alhussaini *et al.*, 2025; Nandini & Selvi, 2025).

In this study, two new Schiff base ligands (HL1 and HL2) were synthesized *via* the condensation of ampicillin with 2-nitrobenzaldehyde and 1-hydroxy-2-naphthaldehyde, respectively. Their corresponding nickel(II) and copper(II) complexes were prepared and characterized using melting point analysis, solubility, molar conductivity, FTIR, UV-Visible spectroscopy, elemental microanalysis, mass spectrometry, and NMR spectroscopy. The antimicrobial activities of the synthesized compounds were evaluated against selected Gram-positive and Gram-negative bacteria, as well as a fungal strain, to assess the influence of metal coordination on biological performance. This work provides insight into the structure–activity relationships of ampicillin-derived Schiff base ligands and their metal complexes, with potential relevance in the development of improved antimicrobial agents.

Experimental

Chemicals and Reagents

All chemicals and solvents used in this study were of analytical grade and were used without further purification unless otherwise stated. Ampicillin trihydrate, 2-nitrobenzaldehyde, 1-hydroxy-2-naphthaldehyde, nickel(II)chloride hexahydrate and copper(II)chloride dihydrate were obtained from Sigma-Aldrich and Merck. Ethanol, methanol, dimethyl sulfoxide (DMSO), chloroform, diethyl ether, n-hexane, and acetone were procured from BDH Chemicals and used as received.

Synthesis of the Schiff base Ligands

Synthesis of HL1

The ligand HL1 was synthesized following a modified literature procedure as reported by (Albotani *et al.*, 2025; Wasafa *et al.*, 2023; Waziri *et al.*, 2023). Ampicillin (1.0 g, 2.5 mmol, 1.0 eq) was dissolved in 30 mL of methanol with continuous stirring. A separate methanolic solution of 2-nitrobenzaldehyde

(0.38 g, 2.5 mmol, 1.0 eq) in 20 mL of methanol was prepared and added dropwise to the ampicillin solution, followed by the addition of three drops of concentrated H_2SO_4 as a catalyst. The reaction mixture was refluxed at 65 °C for 3 hours. Upon completion, the resulting precipitate was collected by filtration, washed with cold methanol, and dried in a desiccator over fused $CaCl_2$. The percentage yield of the product was calculated using the standard procedure, and the compound was subsequently characterized using physicochemical and analytical techniques. The synthetic route for HL1 is presented in **Scheme 1**

.

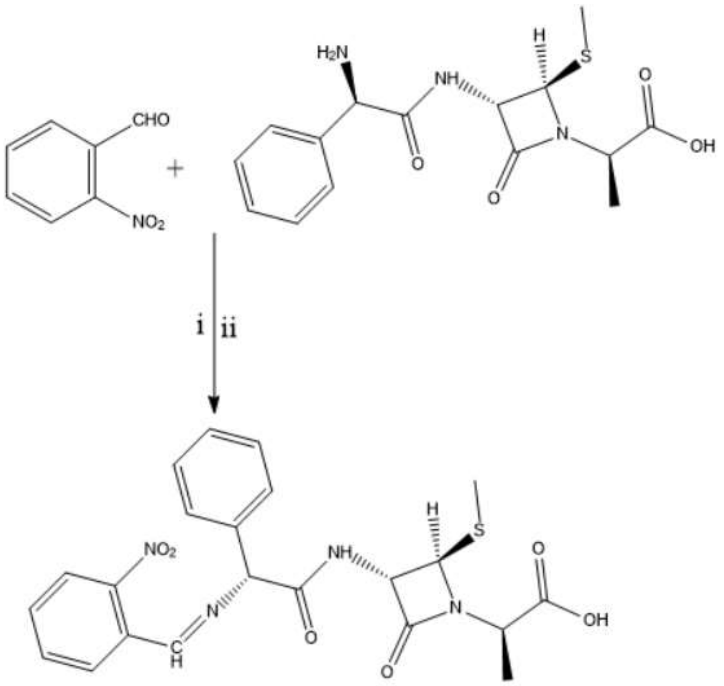

Scheme 1: Pathway for the synthesis of HL1; i = CH_3OH/H_2SO_4, ii = 65 ^oC/3 hours

White solid powder, yield (0.84 g, 57%), m.p. 163-164 °C;UV-Vis (DMSO, 10^{-3} M) λ_{max} (nm): 230 ($\pi \rightarrow \pi^*$), 360 ($n \rightarrow \pi^*$); $FTIR_{ATR}$; U(cm^{-1}): 3350 (N-H), 3100 (O-H), 2920 (C-H), 1720 (C=O), 1620 (C=N), 1520 (N-O), 1350 (C-N), 1276 (C-O), Elemental composition (CHN): Calculated for $C_{22}H_{22}N_4O_6S$; C, 56.16, H, 4.71, N, 11.91, Experimentally obtained for $C_{22}H_{22}N_4O_6S$; C, 56.13, H, 4.74, N, 11.88; Molecular weight for $C_{22}H_{22}N_4O_6S$, *m/z*: Calculated = 493.1245 $[M+Na]^+$, Experimentally obtained = 493.3475 $[M+Na]^+$.

Synthesis of HL2

The ligand HL2 was synthesized using the same modified literature procedure as described for HL1. Ampicillin (1.0 g, 2.5 mmol, 1.0 eq) was dissolved in 30 mL of methanol with continuous stirring. A separate solution of 1-hydroxy-2-naphthaldehyde (0.43 g, 2.5 mmol, 1.0 eq) in 20 mL of methanol was prepared and added dropwise to the ampicillin solution, followed by the addition of three drops of concentrated H_2SO_4 to catalyzed the condensation reaction. The reaction mixture was refluxed at 65 °C for 3 hours. The solid product obtained was filtered, washed with cold methanol, and dried in a desiccator over fused $CaCl_2$. The percentage yield was determined, and the ligand was characterized using standard physicochemical and analytical techniques. The synthetic pathway for HL2 is illustrated in **Scheme 2.**

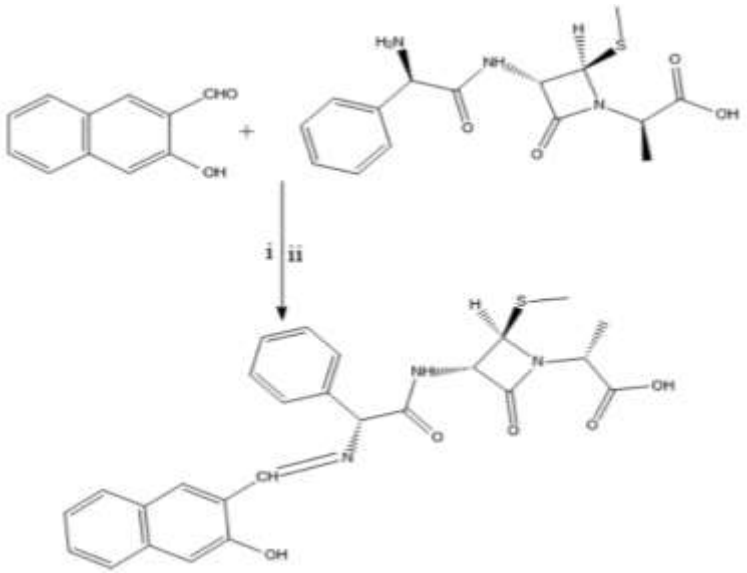

Scheme 2: Pathway for the synthesis of HL2; i = CH_3OH/H_2SO_4, ii = 65 ^oC/3 hours

Milky solid powder, yield (0.90 g, 40%), melting point :183-184^o C; UV-Vis (DMSO, 10^{-3} M) λ_{max} (nm): 265 ($\pi \rightarrow \pi^*$), 384 ($n \rightarrow \pi^*$); $FTIR_{ATR}$; U(cm^{-1}): 3420 (N-H), 3150 (O-H), 2924 (C-H), 1700 (C=O), 1602 (C=N), 1520 (N-O), 1380 (C-N), 1288 (C-O), Elemental composition (CHN): Calculated for$C_{26}H_{25}N_3O_5S$; C, 63.53, H, 5.13, N, 8.55, Experimentally obtained for $C_{26}H_{25}N_3O_5S$; C, 63.48, H, 5.11, N, 8.53; Molecular weight for $C_{26}H_{25}N_3O_5S$, *m/z*: Calculated = 493.1752 $[M+Na]^+$, Experimentally obtained = 493.3616 $[M+Na]^+$.

Synthesis of the Complexes

Synthesis of HL1 Derived Complexes

The HL1-based metal complexes were synthesized following a modified literature procedure (Banbela *et al.*, 2025; Subitha *et al.*, 2021). Briefly, HL1 (1.88 g, 4 mmol, 2 equiv.) was weighed and dissolved in 20 mL of methanol in two separate reaction flasks. Subsequently, solutions of $NiCl_2 \cdot 6H_2O$ (0.47 g, 2 mmol, 1 equiv.) or $CuCl_2 \cdot 4H_2O$ (0.41 g, 2 mmol, 1 equiv.), each prepared in 20 mL of methanol, were added individually to the respective flasks containing the ligand solutions.

Each reaction mixture was refluxed at 65 °C for four hours. The resulting precipitates formed during reflux were collected by gravity filtration, washed thoroughly with methanol to remove any unreacted species, and dried in a desiccator over fused calcium chloride. The obtained complexes were subjected to spectroscopic and analytical characterization for structural confirmation. The reaction pathway for the synthesis of the complexes is illustrated in **Scheme 3.**

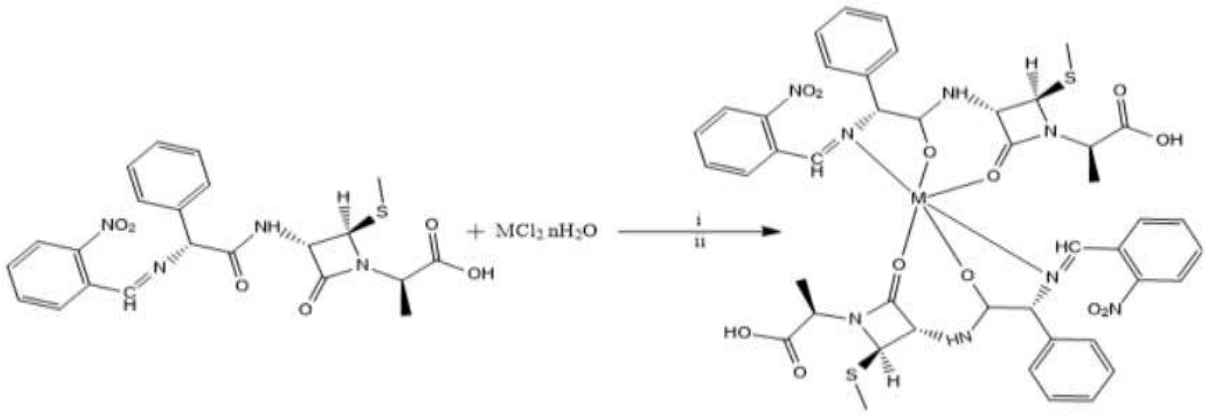

Scheme 3: Pathway for the Synthesis of HL1 Derived Complexes; i = CH_3OH ii = 65 ^oC/3 hours, M = Ni or Cu, n = 4 or 6

NiL1 Complex

Green solid powder, yield: (0.3 g, 61.4 %), m.p, 261-265°C; UV-Vis (DMSO, 10^{-3} M) λ_{max} (nm): 245 ($\pi \rightarrow \pi^*$), 340 ($n \rightarrow \pi^*$); 580 ($d \rightarrow d$);$FTIR_{ATR}$; U(cm^{-1}): 3300 (N-H), 3000 (O-H), 2900 (C-H), 1590 (C=N), 1500 (N-O), 1320 (C-N), 1260 (C-O), 540 (Ni-O), 470 (Ni-N); Elemental composition (CHN): Calculated for $C_{45}H_{49}N_8NiO_{12}S_2$; C, 53.16, H, 4.86, N, 11.02, Experimentally obtained for $C_{45}H_{49}N_8NiO_{12}S_2$; C, 56.13, H, 4.81, N, 10.98.

CuL1 Complex

Blue solid powder, yield:(0.10g, 86%),m.p.283-286 °C; UV-Vis (DMSO, 10^{-3} M) λ_{max} (nm): 233 ($\pi \rightarrow \pi^*$), 325 ($n \rightarrow \pi^*$); 520 (LMCT); $FTIR_{ATR}$; U(cm^{-1}): 3250 (N-H), 3060 (O-H), 2850 (C-H), 1589 (C=N), 1510 (N-O), 1330 (C-N), 1248 (C-O), 529 (Cu-O), 456 (Cu-N); Elemental composition (CHN): Calculated for $C_{45}H_{49}CuN_8O_{12}S_2$; C, 52.91, H, 4.83, N, 10.97, Experimentally obtained for $C_{45}H_{49}CuN_8O_{12}S_2$; C, 52.88, H, 4.81, N, 10.93.

Synthesis of HL2 Derived Complexes

The Ni(II) and Cu(II) complexes of HL2 were synthesized following the same general procedure used for the HL1-derived complexes. Briefly, HL2 (1.97 g, 4 mmol, 2 equiv.) was weighed and dissolved in 20 mL of methanol in two separate reaction flasks. Solutions of $NiCl_2 \cdot 6H_2O$ (0.47 g, 2 mmol, 1 equiv.) and $CuCl_2 \cdot 4H_2O$ (0.41 g, 2 mmol, 1 equiv.), each prepared in 20 mL of methanol, were added individually to the respective flasks containing the ligand solutions.

Each reaction mixture was refluxed at 65 °C for four hours. The resulting precipitates formed during reflux were collected by gravity filtration, washed with cold methanol to remove unreacted starting materials, and dried in a desiccator over fused calcium chloride. The obtained complexes were subsequently analysed using spectroscopic and analytical techniques for structural confirmation. The reaction pathway leading to the formation of the complexes is illustrated in **Scheme 4**.

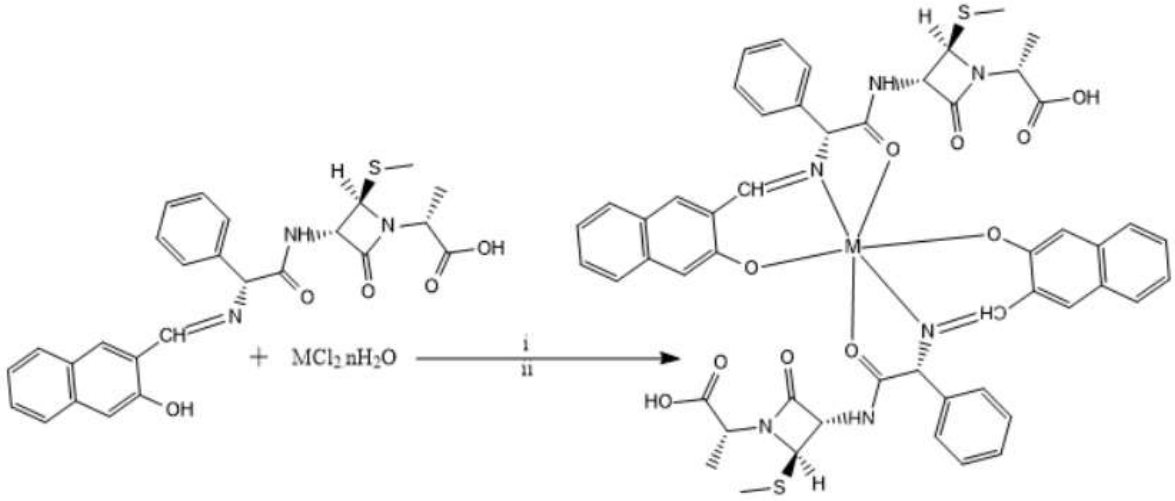

Scheme 4: Pathway for the Synthesis of HL2 Derived Complexes; i = CH_3OH ii = 65 ^oC/3 hours, M = Ni or Cu, n = 4 or 6

NiL2 Complex

Green solid powder, yield: (0.20 g, 53.2 %), m.p, 256-258°C; UV-Vis (DMSO, 10^{-3} M) λ_{max} (nm): 225 ($\pi \rightarrow \pi^*$), 330 ($n \rightarrow \pi^*$); 560 ($d \rightarrow d$); $FTIR_{ATR}$; U(cm^{-1}): 3310 (N-H), 3100 (O-H), 2900 (C-H), 1585 (C=N), 1345 (C-N), 1240 (C-O), 535 (Ni-O), 462 (Ni-O); Elemental composition (CHN): Calculated for $C_{52}H_{48}N_6NiO_{10}S_2$; C, 60.07, H, 4.65, N, 8.08, Experimentally obtained for $C_{52}H_{48}N_6NiO_{10}S_2$; C, 60.03, H, 4.61, N, 8.05.

CuL2 Complex

Blue solid powder, yield: (0.16 g, 64.3%), m.p. 273-275°C; UV-Vis (DMSO, 10^{-3} M) λ_{max} (nm): 245 ($\pi \rightarrow \pi^*$), 360 ($n \rightarrow \pi^*$); 490 (LMCT); $FTIR_{ATR}$; U(cm^{-1}): 3300 (N-H), 3090 (O-H), 2800 (C-H), 1580 (C=N),1351 (C-N), 1250 (C-O), 528 (Cu-O), 463 (Cu-N); Elemental composition (CHN): Calculated for $C_{52}H_{48}CuN_6O_{10}S_2$; C, 59.79, H, 4.63, N, 8.04, Experimentally obtained for $C_{52}H_{48}CuN_6O_{10}S_2$; C, 59.73, H, 4.58, N, 7.98.

Measurements and Instrumentation

All spectroscopic and analytical measurements were performed using standard instrumentation. The FT-IR spectra of the ligand and its complexes were recorded in the solid state using a Bruker Tensor 27 FT-IR spectrometer and a PerkinElmer BX FT-IR spectrometer over the range 4000–400 cm^{-1}. Elemental (CHN) analysis was conducted using a Vario EL III Elementar microanalyzer to determine the percentage composition of carbon, hydrogen, and nitrogen. UV–Visible spectra were obtained on a PerkinElmer UV–Vis spectrophotometer in the wavelength range of 200–800 nm at room temperature, using 10^{-3} M solutions of the samples prepared in DMSO.

Antimicrobial Study

The antibacterial and antifungal activities of the free ligands (HL1 and HL2) and their corresponding Nickel and Copper complexes were evaluated in comparison with ampicillin using the disc diffusion method (Alshater *et al.,* 2023; Zalevskaya & Gur'eva, 2021). The test organisms included two Gram-positive bacteria (*Staphylococcus aureus* and *Streptococcus pyogenes*), two Gram-negative bacteria (*Salmonella typhi* and *Escherichia coli*), and one fungal strain (*Candida albicans*). Fresh microbial suspensions were prepared in nutrient agar medium, poured into sterile Petri dishes, and allowed to solidify. Solutions of the test compounds (30, 20, and 10 mg/mL in methanol) were applied onto sterile discs, with ampicillin serving as the reference standard. The inoculated plates were incubated at 37 °C for 24 hours for bacteria and 48 hours for fungi. Antimicrobial activity was assessed by measuring the diameter of the inhibition zones (mm). Megur (2023). All results are presented as mean ± SEM. Because several compounds produced identical inhibition zones across replicate measurements, statistical variance was minimal; therefore, the antimicrobial data are interpreted descriptively, focusing on relative activity patterns across compounds, concentrations, and microbial strains rather than formal significance testing

Results and Discussion

Synthesis and Physical Properties

The Schiff base ligands HL1 and HL2 were synthesized *via* a condensation reaction between 2-nitrobenzaldehyde and 2-hydroxy-1-naphthaldehyde with penicillin, respectively, in methanolic medium using a catalytic amount of sulfuric acid at 65 °C, as illustrated in Schemes 1 and 2. HL1 was obtained as a white solid powder, while HL2 appeared as a milky solid. The ligands were subsequently reacted with Nickel and Copper ions using their corresponding metal chloride salts in a 1:2 metal-to-ligand molar ratio to afford the complexes (NiL1, CuL1, NiL2, and CuL2). The Nickel complexes were isolated as green solids, whereas the Copper complexes appeared as blue solids colours typical of transition-metal systems due to partially filled d-orbitals and characteristic d→d transitions (Ngece *et al.,* 2025; Yusuf *et al.,* 2021).

The compounds were obtained in moderate yields (40–86%) and were stable to air and moisture. All ligands and complexes were soluble in polar solvents but insoluble in non-polar solvents, indicating their polar nature. In addition, the melting points of the metal complexes were found to be higher than those of the free ligands, consistent with the formation of new coordination entities with higher molecular weights and enhanced lattice stability (Adhikari *et al.,* 2025). Molar conductivity measurements were carried out for the synthesized complexes in 10^{-3} M DMSO solutions at room temperature. The NiL1 and CuL1 complexes exhibited low molar conductivity values of 8.92 and 9.04 Ω^{-1} cm^2 mol^{-1}, respectively, while slightly higher but still low values in the range of 9.6 and 13.6 Ω^{-1} cm^2 mol^{-1} were observed for NiL2 and CuL2. These values fall well within the characteristic range reported for non-electrolytic metal complexes (< 20 Ω^{-1} cm^2 mol^{-1} in DMSO), indicating that the complexes do not dissociate into ions in solution.

The low molar conductivity confirms that no counter-ions (e.g., chloride or acetate) are present outside the coordination sphere and that all anionic donor atoms are coordinated directly to the metal centre. This observation supports the formulation of the complexes as neutral, inner-sphere coordination compounds, consistent with the proposed octahedral geometries derived from spectroscopic analysis.

A summary of the physicochemical properties of the ligands and their complexes is presented in Table 1. Further confirmation of complex formation and coordination behaviour was

obtained through spectroscopic characterization, as discussed in the subsequent sections.

Table 1: Physiochemical Properties of the ligands and their complexes

Compounds	Molecular Formula	Molecular mass	Yield: g(%)	Colour	M.P. °C
HL1	$C_{22}H_{22}N_4O_6S$	470.13	0.84(57.0)	White	163-164
HL2	$C_{26}H_{25}N_3O_5S$	491.15	0.90(40.0)	Milky	183-184
NiL1	$C_{45}H_{49}N_8NiO_{12}S_2$	1015.23	0.30(61.4)	Green	261-265
CuL1	$C_{45}H_{49}CuN_8O_{12}S_2$	1020.22	0.10(86.0)	Blue	283-286
NiL2	$C_{52}H_{48}N_6NiO_{10}S_2$	1038.22	0.20(53.2)	Green	256-258
CuL2	$C_{52}H_{48}CuN_6O_{10}S_2$	1043.22	0.16(64.3)	Blue	273-275

Spectroscopic Characterization

FTIR Spectral Study

The FTIR spectra of the free Schiff bases (HL1 and HL2) and their Ni(II) and Cu(II) complexes (Figures 1-2) provide clear evidence for coordination through the azomethine nitrogen and the amide carbonyl oxygen, while excluding direct involvement of the amide N–H or carboxylic OH groups. In the spectra of the free ligands, the azomethine ν(C=N) stretching vibration appears at approximately 1620 cm^{-1} and undergoes a systematic shift to lower wavenumbers (≈1589–1590 cm^{-1}) upon complexation, consistent with coordination of the imine nitrogen to the metal centre via lone-pair donation and formation of an M–N bond.

Notably, the amide ν(C=O) stretching band observed in the free ligands is no longer resolved at its original position in the metal complexes. This behaviour does not indicate loss of the amide functionality; rather, coordination of the carbonyl oxygen to the metal reduces the C=O bond order through electron donation, leading to band weakening, broadening, and overlap with neighbouring vibrations, such that the free ligand ν(C=O) band becomes indistinguishable in the complex spectra. This spectral change is characteristic of amide oxygen coordination in metal–Amide systems (Elbadawy *et al.*, 2025).

In contrast, the broad N–H/O–H stretching envelope in the 3420–3000 cm^{-1} region persists in both Ni(II) and Cu(II) complexes with only minor changes in shape and position, confirming that neither the amide N–H nor the carboxylic OH groups are deprotonated or directly involved in metal binding. The retention of the amide N–H vibration, together with the altered carbonyl region, supports a coordination mode in which the amide oxygen acts as a neutral donor while the N–H bond remains intact, consistent with established coordination behaviour of amide-containing ligands. This observation is corroborated by the relatively unchanged phenolic ν(C–O) band (~1270 cm^{-1}) in the complexes (Leveraro *et al.*, 2025).

Finally, new absorptions in the low-frequency region (≈540–528 cm^{-1} and ≈470–462 cm^{-1}) appear in the spectra of Nickel and Copper derivatives and are assigned to ν(M–O) and ν(M–N) vibrations, respectively (Mazen *et al.*, 2021). These bands provide direct spectroscopic evidence for the proposed ONO-tridentate coordination mode in the metal complexes. In this chelation mode, the O-donor originates from the amide carbonyl/β-lactam ring oxygen in HL1 and from the amide carbonyl/hydroxyl oxygen in HL2, while the N-donor corresponds to the azomethine nitrogen of the Schiff base in both ligands. Collectively, the IR results are therefore consistent with formation of neutral chelate complexes in which the ligand binds *via* amide-C=O and azomethine-N, while carboxylic OH and amide NH groups remain uncoordinated (Takalloo *et al.*, 2024). Figure 3, visually highlights the systematic shifts and changes in the key functional group upon complexation, confirming coordination through the amide carbonyl oxygen and azomethine nitrogen atoms.

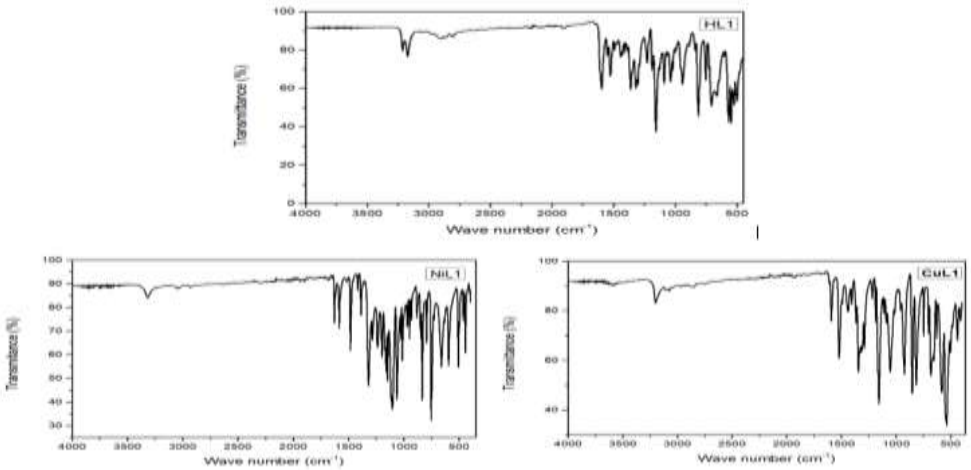

Figure 1: FTIR Spectra of HL1 and its NiL1 and CuL1 complexes obtained in solid state using ATR method

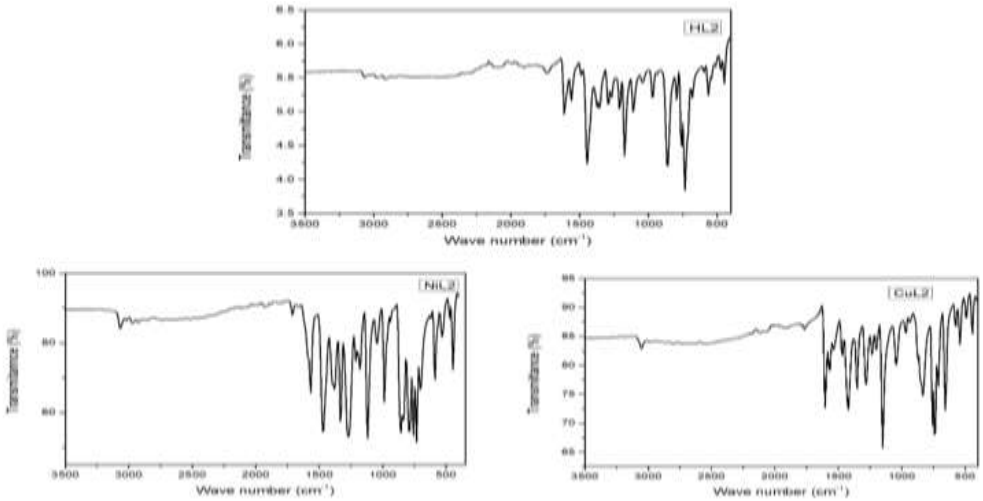

Figure 2: FTIR Spectra of HL2 and its NiL2 and CuL2 complexes obtained in solid state using ATR method

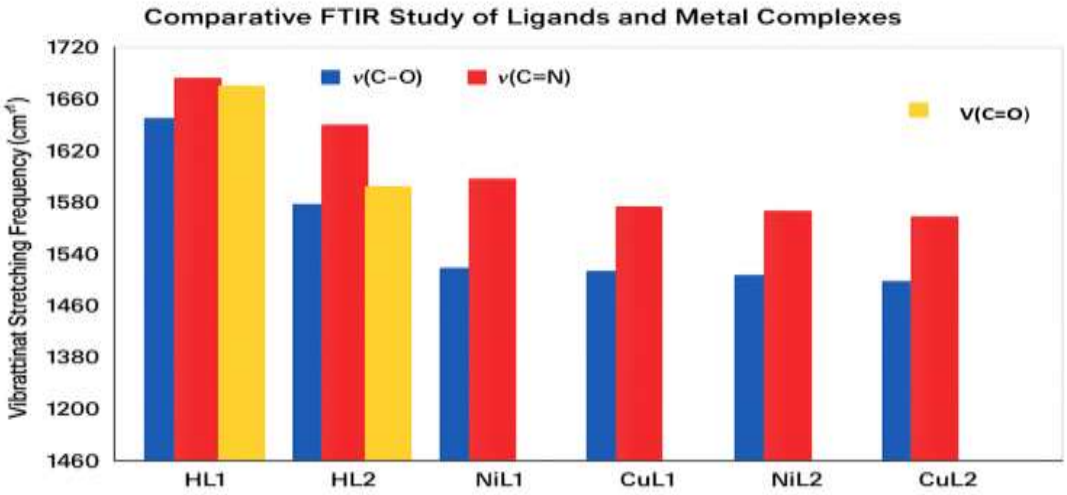

Figure 3: Comparative FTIR data for the ligand and their complexes (selected bands). Key evidence for coordination includes the downshift of the ν(C=N) and ν(C-O) vibration and the disappearance of ν(C=O) vibration band in the complexes.

UV–Visible Spectral Analysis

The UV–Visible spectral data of the ligands (HL1 and HL2) and their corresponding Nickel and Copper complexes (NiL1, CuL1, NiL2, and CuL2) are presented in (Table 2 and Figures 4-5). The free ligands HL1 and HL2 exhibited two major absorption bands in the ultraviolet region, assigned to π→π* and n→π* transitions of the aromatic and azomethine chromophores. The bands observed at 230 and 360 nm for HL1, and at 265 and 384 nm for HL2, are characteristic of conjugated systems containing C=N and phenolic groups. The bathochromic shift observed in HL2 relative to HL_1 is attributed to extended π-conjugation within the naphthyl moiety (Chiyindiko *et al.*, 2022).

Upon coordination with Ni(II) and Cu(II) ions, the electronic spectra of the complexes show systematic changes relative to the free ligands, reflecting metal–ligand orbital interactions. In all complexes, the ligand-cantered π→π* and n→π* transitions undergo moderate shifts compared to the free Schiff bases, confirming coordination through the azomethine nitrogen and amide carbonyl oxygen atoms. For NiL1 and CuL1, these transitions appear at 245/340 nm and 233/325 nm, respectively, while for NiL2 and CuL2 they are observed at 225/330 nm and 245/350 nm. Such shifts are consistent with ligand-to-metal charge redistribution and partial delocalization of electron density upon complex formation, leading to a reduction in the ligand-cantered energy gap (Mujahid *et al.*, 2023).

In addition to these ligand-cantered transitions, all complexes exhibit new, lower-energy absorption bands in the visible region, 580 nm (NiL1), 520 nm (CuL1), 560 nm (NiL2), and 490 nm (CuL2), which are absent in the spectra of the free ligands. These bands are characteristic of metal-cantered electronic transitions and/or charge-transfer processes and therefore provide strong evidence for coordination. For the Ni(II) complexes, which possess a d^8 electronic configuration, the observed visible bands are reasonably assigned to spin-allowed d–d transitions expected for octahedral or distorted octahedral environments, possibly with some contribution from ligand-to-metal charge transfer (LMCT), as commonly reported for Schiff base–Ni(II) systems (Halid, 2016).

For the Cu(II) complexes (d^9), the visible bands are best interpreted as arising from a combination of d–d transitions and significant LMCT character. In octahedral or pseudo-octahedral Cu(II) systems, strong Jahn–Teller distortion is expected, leading to axial elongation and pronounced splitting of the eg and t2g orbitals. As a result, Cu(II) d–d transitions are often broadened, shifted to higher energies, and partially obscured by LMCT bands. The relatively blue-shifted visible absorptions observed for CuL1 and CuL2 compared to their Ni(II) analogues are therefore consistent with Jahn–Teller-induced orbital splitting and enhanced charge-transfer contributions, rather than purely ligand-field transitions (Halid, 2016; Marlina, 2015).

The calculated transition energies for the visible bands (V_3) follow the order: CuL2 (2.531 eV) > CuL1 (2.385 eV) > NiL2 (2.214 eV) > NiL1 (2.138 eV) (Table 3). This trend indicates that the Cu(II) complexes absorb at higher energies (shorter wavelengths) than the corresponding Ni(II) complexes, consistent with stronger metal–ligand interactions, Jahn–Teller distortion effects in Cu(II), and/or greater LMCT contributions. The higher transition energy of CuL2 relative to CuL1 further suggests that the L2 ligand framework imposes a slightly stronger ligand field or facilitates greater orbital overlap, in agreement with the observed IR and UV–Vis spectral differences between the ligands (Santos *et al.*, 2025).

Table 2: UV–Visible absorption data for the ligands and their complexes

Compound	V_1 (nm)	V_2 (nm)	V_3 (nm)	Tentative Assignment
HL1	230	277	360	π→π* and n→π* (C=N, aromatic)
HL2	265	384	–	π→π* and n→π* (C=N, naphthyl system)
NiL1	245	340	580	π→π*, n→π*, d–d/LMCT transition
CuL1	245	370	520	π→π*, n→π*, d–d/LMCT transition
NiL2	225	330	560	π→π*, n→π*, d–d/LMCT transition
CuL2	245	350	490	π→π*, n→π*, d–d/LMCT transition

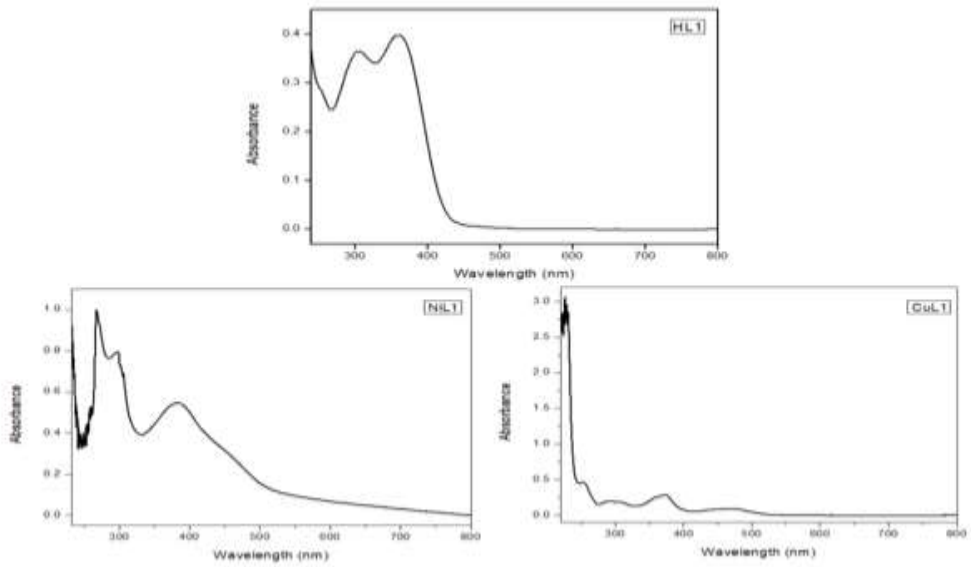

Figure 4: UV-Vis Spectra of HL1 and it NiL1 and CuL1 Complexes recorded in DMSO (10^{-3} M) solution at room temperature

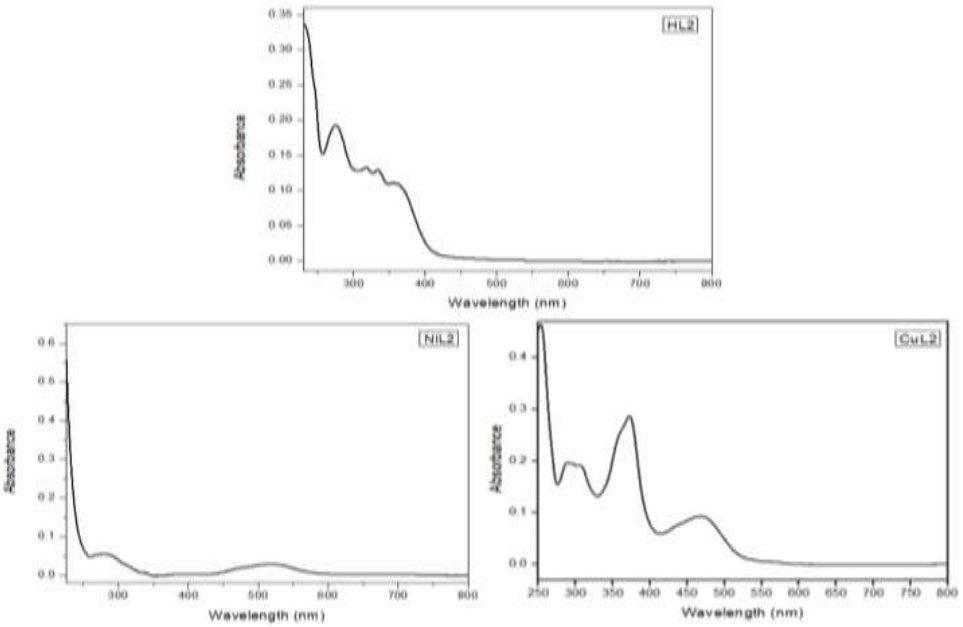

Figure 5: UV-Vis Spectra of HL2 and it NiL2 and CuL2 Complexes recorded in DMSO (10^{-3} M) solution at room temperature

Table 3: LMCT/d–d transition wavelengths (λ_3) and corresponding transition energies (eV) for the complexes

Complex	λ_3 (nm)	Energy (eV)
NiL1	580	2.1379 eV
CuL1	520	2.3846 eV
NiL2	560	2.2143 eV
CuL2	490	2.5306 eV

Elemental Analysis and Mass spectral study

The elemental (CHN) analytical data for the ligands and their metal complexes, together with the mass spectral data of the ligands (Table 4), showed excellent agreement between the experimentally determined and theoretically calculated values. This concordance confirms the expected molecular

compositions and the high purity of the synthesized compounds. The calculated and found percentages of carbon, hydrogen, and nitrogen exhibit only minimal deviations for all samples, strongly supporting the successful synthesis of the penicillin-based Schiff base ligands (HL1 and HL2) and their corresponding nickel and copper complexes. The close alignment between theoretical and experimental values indicates negligible analytical variation, affirming both the stoichiometric correctness and the homogeneity of the synthesized compounds. Although, a noticeable variation exist between the experimental and theoretical composition of carbon in NiL2. The slightly higher experimental carbon content observed compared to the calculated value is attributed to trace inclusion of residual organic solvent or adventitious carbon, a well-documented phenomenon in coordination compounds. Notably, the hydrogen and nitrogen values are in good agreement with the calculated composition.

Table 4: Comparison of calculated and experimentally found elemental (CHN) compositions for the ligands and their complexes.

Compound	Calculated			Experimental		
	C	H	N	C	H	N
HL1	56.16	4.71	11.91	56.13	4.74	11.88
HL2	63.53	5.13	8.55	63.48	5.11	8.53
NiL1	53.16	4.86	11.02	56.13	4.81	10.98
CuL1	52.91	4.83	10.97	52.88	4.81	10.93
NiL2	60.07	4.65	8.08	60.03	4.61	8.05
CuL2	59.79	4.63	8.04	59.73	4.58	7.98

Antimicrobial Study

Having successfully confirmed the formation of the ligands and their complexes as detailed in the characterization section above. The ligands and their metal complexes were evaluated as a potential antimicrobial agent. The antimicrobial activities of the Schiff base ligands (HL1 and HL2) and their nickel and copper complexes were evaluated against a panel of Gram-positive bacteria (*Staphylococcus aureus* and *Streptococcus pyogenes*), Gram-negative bacteria (*Escherichia coli* and *Salmonella typhi*), and the fungal strain *Candida albicans*. The results obtained at test concentrations of 30, 20, and 10 µg/mL are summarized in Tables 5–7, respectively.

At 30 µg/mL (Table 5), both ligands and several metal complexes exhibited selective activity against Gram-positive strains, while activity against Gram-negative bacteria and fungi was largely absent. HL1 and HL2 both show strong activity against *S. pyogenes* (30 mm each) with moderate activity of HL1 against *S. aureus* (13 mm). Metalation alters the activity profile: CuL1 and NiL1 show enhanced *S. aureus* activity (18 and 17 mm, respectively) compared with their free ligands, while CuL2 uniquely shows measurable activity against *E. coli* (16 mm) at 30 µg/mL, a notable gain of Gram-negative potency relative to other complexes. Ampicillin profile at the same concentration is broadly comparable for *S. aureus* and *E. coli* (≈15–17 mm) and superior for *S. typhi* (24 mm). At 20 µg/mL (Table 6) activity decreases overall but trends persist: HL1 retains activity against *S. aureus* and *S. pyogenes*, while NiL1 and CuL1 continue to show measurable zones against Gram-positive strains; CuL2 uniquely retains some *E. coli* activity (10 mm) at 20 µg/mL. At 10 µg/mL (Table 7) only a subset of complexes remain active: CuL1 and NiL1 each retain modest activity against *S. aureus* (7 mm), and NiL1 shows activity against *S. pyogenes* (7 mm), highlighting that NiL1 and CuL1 possess the best retained potency on dilution. Across the dataset, metal complexation (particularly Ni and Cu) generally increases activity against Gram-positive strains relative to free ligands and provides the only examples of measurable Gram-negative activity (CuL2). HL1 (ampicillin-derived with 2-nitrobenzaldehyde) and HL2 (ampicillin-derived with 2-hydroxy-1-naphthaldehyde) show complementary behaviour: HL1 is overall more active against *S. aureus* while HL2 tracks well for *S. pyogenes* at higher concentrations. Taken

together, NiL1 and CuL1 are the lead complexes for retained broad Gram-positive potency at lower dose; CuL2 is notable for its unique Gram-negative activity (against *E. coli*). These results suggest the metal centre and specific ligand substituents modulate membrane/permeation or redox-mediated mechanisms that selectively affect Gram-positive organisms, while certain ligand–metal combinations (CuL2) may favour Gram-negative penetration or specific target engagement (Sharma *et al.*, 2022).

Table 5: Zone of inhibition (mm) of ligands and metal complexes at 30 µg/mL

Compound	*S. aureus*	*S. pyogenes*	*E. coli*	*S. typhi*	*C. albicans*
HL1	13 ± 0.00	30 ± 0.00	0 ± 0.00	0 ± 0.00	0 ± 0.00
HL2	10 ± 0.00	30 ± 0.00	0 ± 0.00	0 ± 0.00	0 ± 0.00
CuL1	18 ± 0.00	14 ± 0.00	0 ± 0.00	0 ± 0.00	0 ± 0.00
CuL2	12 ± 0.00	20 ± 0.00	16 ± 0.00	0 ± 0.00	0 ± 0.00
NiL1	17 ± 0.00	17 ± 0.00	0 ± 0.00	0 ± 0.00	0 ± 0.00
NiL2	13 ± 0.00	0 ± 0.00	0 ± 0.00	0 ± 0.00	0 ± 0.00
Amp	15.3±2.00	0±0.00	17.0±2.00	24.±4.67	NA
DMSO	-	-	-	-	-

Note: Amp = Ampicillin and NA = Not applicable

Table 6: Zone of inhibition (mm) of ligands and metal complexes at 20 µg/mL

Compound	*S. aureus*	*S. pyogenes*	*E. coli*	*S. typhi*	*C. albicans*
HL1	8 ± 0.00	23 ± 0.00	0 ± 0.00	0 ± 0.00	0 ± 0.00
HL2	0 ± 0.00	24 ± 0.00	0 ± 0.00	0 ± 0.00	0 ± 0.00
CuL1	13 ± 0.00	8 ± 0.00	0 ± 0.00	0 ± 0.00	0 ± 0.00
CuL2	7 ± 0.00	14 ± 0.00	10 ± 0.00	0 ± 0.00	0 ± 0.00
NiL1	12 ± 0.00	12 ± 0.00	0 ± 0.00	0 ± 0.00	0 ± 0.00
NiL2	7 ± 0.00	0 ± 0.00	0 ± 0.00	0 ± 0.00	0 ± 0.00
Amp	13.0±1.53	0±0.00	16.6±.5.69	21.3±2.65	NA
DMSO	-	-	-	-	-

Table 7: Zone of inhibition (mm) of ligands and metal complexes at 10 µg/mL

Compound	S. aureus	S. pyogenes	E. coli	S. typhi	C. albicans
HL1	0 ± 0.00	16 ± 0.00	0 ± 0.00	0 ± 0.00	0 ± 0.00
HL2	0 ± 0.00	0 ± 0.00	0 ± 0.00	0 ± 0.00	0 ± 0.00
CuL1	7 ± 0.00	0 ± 0.00	0 ± 0.00	0 ± 0.00	0 ± 0.00
CuL2	0 ± 0.00	8 ± 0.00	0 ± 0.00	0 ± 0.00	0 ± 0.00
NiL1	7 ± 0.00	7 ± 0.00	0 ± 0.00	0 ± 0.00	0 ± 0.00
NiL2	0 ± 0.00	0 ± 0.00	0 ± 0.00	0 ± 0.00	0 ± 0.00
Amp	12.00±2.52	0±0.00	16.0±1.00	18.0±2.08	-
DMSO	-	-	-	-	-

Proposed Mechanism of Antimicrobial Activity

The enhanced antimicrobial activity of the nickel and copper Schiff base complexes is likely governed by a combination of chelation-driven physicochemical changes and metal-assisted biochemical interactions. Chelation reduces the polarity of the metal ion through partial charge redistribution with the ligand, increasing lipophilicity and facilitating penetration through microbial cell membranes. Once inside the cell, the complexes may interact with intracellular targets via multiple pathways. The presence of the azomethine (–C=N) linkage and aromatic π-systems allows strong π–π and hydrogen-bonding interactions with DNA bases, potentially interfering with replication and transcription. Additionally, copper and nickel, being redox-active and borderline Lewis's acids, may catalyze the generation of reactive oxygen species (ROS) through ligand-to-metal charge transfer (LMCT) or redox cycling, leading to oxidative damage of proteins, lipids, and nucleic acids. Metal binding to key enzymatic thiol groups or active-site residues may further disrupt metabolic pathways. Collectively, these synergistic effects, membrane permeation,

DNA/protein binding, ROS generation, and enzyme inhibition, likely contribute to the observed broad-spectrum antimicrobial activity of the complexes (Babu & Ayodhya, 2023).

Structural Activity Relationship (SARS)

The antibacterial data indicate a clear SAR in which both ligand electronics/size and metal identity strongly modulate bioactivity. Complexation of the Schiff base ligands consistently improved potency relative to the free ligands (Tables 6–8), showing that chelation is a primary driver of activity: coordination lowers overall polarity through partial charge delocalization between metal and donor atoms, increasing lipophilicity and membrane permeation. Between the two ligand frameworks, HL2 (the 2-hydroxy-1-naphthyl derivative) produced more active complexes than the HL1 (2-nitrophenyl) analogue, most notably CuL2, which alone inhibited *E. coli*. This is consistent with HL2's larger π-surface and greater hydrophobicity, which facilitate stronger π–π/van-der-Waals interactions with membrane components and cellular targets and improve complex uptake. The superior performance of copper complexes (especially CuL2) relative to nickel counterparts points to a metal-centred contribution: copper, a borderline Lewis acid, matches well with the N,O donor set and can participate in facile ligand-to-metal charge transfer (LMCT) or redox mediation, enhancing electron-transfer based mechanisms (e.g., localized oxidative stress or redox cycling) that augment bactericidal action. In HSAB terms, copper's borderline softness provides stronger covalent character with the Schiff donor set than nickel, leading to more stable, lipophilic complexes that better traverse Gram-negative barriers. Finally, ligand-field/d–d and LMCT perturbations alter the electronic distribution of the complex and thereby its ability to interact non-covalently and coordinate to biomolecular targets; complexes showing notable LMCT/d–d features (CuL2, NiL1) correlate with the lowest MICs. Collectively, these observations suggest that optimizing ligand π-conjugation and selecting borderline-soft metal centres (e.g., Cu) are promising strategies to increase antimicrobial potency in this Schiff-base family (Nagajothi & Maheswari, 2021).

Conclusion

In this study, two Schiff base ligands (HL1 and HL2) were successfully synthesized from ampicillin through condensation with 2-nitrobenzaldehyde and 2-hydroxy-1-naphthaldehyde, respectively, and coordinated with nickel and copper ions to afford four new complexes (NiL1, CuL1, NiL2, and CuL2). Comprehensive physicochemical and spectroscopic analyses, including FTIR, UV–Vis, elemental analysis, melting point, solubility tests, and NMR, confirmed the successful formation of the ligands and their corresponding metal complexes. Infrared and electronic spectral data revealed the expected coordination through the azomethine nitrogen and the carbonyl oxygen of the amide group, accompanied by characteristic shifts in ν(C=N), ν(C–O), and ν(C=O) that clearly support metal–ligand chelation. The enhanced thermal stability, distinctive spectral signatures, and analytical consistency further validated the proposed structures. Biological evaluation demonstrated that complexation significantly improved the antimicrobial properties of the ligands. While HL1 and HL2 displayed activity only against Gram-positive bacteria at higher concentrations, their metal complexes, particularly CuL2 and NiL1, exhibited broader and more potent activity profiles, including measurable inhibition of *E. coli*. These findings are consistent with established chelation-enhancement principles, where increased lipophilicity and favourable metal–ligand electronic interactions facilitate improved membrane penetration and target binding. The structure–activity relationship (SAR) analysis highlights the beneficial roles of π-conjugation, ligand hydrophobicity, and metal identity (Cu > Ni) in modulating antimicrobial efficacy. Overall, this work demonstrates that ampicillin-derived Schiff bases and their nickel/copper complexes constitute promising chemical scaffolds with enhanced antimicrobial potential. The insights obtained from their synthesis, coordination behaviour, and biological performance provide a valuable foundation for future optimization, including mechanistic studies, computational modelling, and exploration of additional metal ions, to support the development of next-generation metal-based antimicrobial agents.

Authors Contributory Statements

All authors contributed substantially to the conception, design, and execution of the

research work. Experimental synthesis, characterization studies, and data acquisition were carried out by M. B. Mshelia as part of his M.Sc. research project at the Department of Pure and Applied Chemistry, University of Maiduguri, Borno State, Nigeria. Data interpretation, manuscript drafting, critical review, and editing were jointly performed by all authors. All authors have read and approved the final version of the manuscript.

Conflict of Interest Statements

The authors declare that they have no known financial or personal conflicts of interest that could have influenced the work reported in this manuscript.

Reference

Shafie, Alaa, & Ashour, Amal Adnan. (2025). Recent advances in Schiff bases and Cu (II) complexes: Applications in fluorescence imaging and anticancer therapy (2020–2024). *Journal of Inorganic Biochemistry*, 112909.

Adhikari, Janak, Bhattarai, Ajaya, & Chaudhary, Narendra Kumar. (2025). Synthesis, characterization, and antibacterial assessment of Homo-and binuclear transition metal complexes of surfactant-based N, N-donor Schiff base. *Results in Chemistry*, 102421.

Al-Noor, Taghreed H, Mohapatra, Ranjan K, Azam, Mohammad, Karem, Lekaa K Abdul, Mohapatra, Pranab K, Ibrahim, Abeer A, Al-Resayes, Saud I. (2021). Mixed-ligand complexes of ampicillin derived Schiff base ligand and Nicotinamide: Synthesis, physico-chemical studies, DFT calculation, antibacterial study and molecular docking analysis. *Journal of Molecular Structure*, *1229*, 129832.

Albotani, Asem SA, Mohammed, Eman R, Al-Dulaimi, Muna S, Saied, Shakir M, & Saleh, Mohaned Y. (2025). Synthesis, Characterization, In Silico Screening for Molecular Docking and Computational Exploration of Some Novel Metal Complexes Derived from Ampicillin-Isatine Schiff Bases. *New Mater. Compd. Appl.*, *9*, 109-122.

Alhussaini, MS, Alyahya, AAI, & Al-Ghanayem, AA. (2025). Antimicrobial Applications of Fe (II) and Fe (III) Schiff Base Complexes: Role of Complexation in Activity Enhancement: A Review (2020–2025). *Russian Journal of Coordination Chemistry*, 1-13.

Alshater, Heba, Al-Sulami, Ahlam I, Aly, Samar A, Abdalla, Ehab M, Sakr, Mohamed A, & Hassan, Safaa S. (2023). Antitumor and antibacterial activity of Ni (II), Cu (II), Ag (I), and Hg (II) complexes with ligand derived from thiosemicarbazones: Characterization and theoretical studies. *Molecules*, *28*(6), 2590.

Arshi, Farha, Bano, Swaila, Singh, Ashok, Firdaus, Saniya, Kumar, Saurabh, Banerjee, Monisha, Singh, Sudheer K. (2023). Ampicillin-Derived Ruthenium Schiff Base Complexes as Emerging Anticancer and Antimicrobial Candidates: Synthesis, Characterization, DFT, ADME and Molecular Docking. *Characterization, DFT, ADME and Molecular Docking. Journal of Molecular Structures*, 2, 23451

Babu, K Jagadesh, & Ayodhya, Dasari. (2023). Comprehensive investigation of Co (II), Ni (II) and Cu (II) complexes derived from a novel Schiff base: synthesis, characterization, DNA interactions, ADME profiling, molecular docking, and in-vitro biological evaluation. *Results in Chemistry*, *6*, 101110.

Banbela, Hadeel M, Al-Dahiri, Reema H, Abubakr, Amrajaa S, Hassan, Safaa S, & Mohamed, Magda. (2025). Amoxicillin Antibiotic with Potential Anticancer and Antidiabetic Activity: Acetaldehyde-Amoxicillin Schiff Base and Its Vanadyl Complex with DFT and Docking Investigation. *Materials Advances*, 5, 2345.

Bereda, Gudisa. (2022). Clinical pharmacology of ampicillin. *Journal of Pharmaceutical Research & Reports. SRC/JPRSR-141. DOI: doi. org/10.47363/JPRSR/2022 (3), 129*, 8-10.

Chiyindiko, Emmie, Langner, Ernst HG, & Conradie, Jeanet. (2022). Spectroscopic behaviour of copper (II) complexes containing 2-hydroxyphenones. *Molecules*, *27*(18), 6033.

Elbadawy, Hemmat A, Eldissouky, Ali, El-Apasery, Morsy Ahmed, Elsayed, Doaa S, & Alaswad, Entesar A. (2025). Synthesis, characterization, computational and dyeing behavior of Cu (II) and Zn (II) metal complexes derived from azo-Schiff bases

containing phenol derivatives. *BMC chemistry*, *19*(1), 207.

Gambo, SB, Mukhtar, AA, Labaran, HB, Labaran, HB, Mustapha, A, Ibrahim, SI, & Ali, M. (2023). Chemistry, mode of action, bacterial resistance, classification and adverse effects of Beta-lactam antibiotics: a review. *Int. J. Dermatol. Res*, *5*, 11-16.

Halid, Yanti Yana. (2016). *Photonic, Magnetic and Metallomesogenic Properties of Cu (Ii), Ni (Ii), Co (Ii), Fe (Ii) and Mn (Ii)/Mn (Iii) Complexes with Alkylcarboxylates, Schiff Bases and Cyclam as Ligands.* University of Malaya (Malaysia).

Hutskalova, Valeriia, & Sparr, Christof. (2024). Aromatic ring-opening metathesis. *Nature*, 1-2.

Krishna, G Anjali, Dhanya, TM, Shanty, AA, Raghu, KG, & Mohanan, PV. (2023). Transition metal complexes of imidazole derived Schiff bases: Antioxidant/anti-inflammatory/antimicrobial/enzyme inhibition and cytotoxicity properties. *Journal of Molecular Structure*, *1274*, 134384.

Kumar, Binesh, Devi, Jai, & Manuja, Anju. (2023). Synthesis, structure elucidation, antioxidant, antimicrobial, anti-inflammatory and molecular docking studies of transition metal (II) complexes derived from heterocyclic Schiff base ligands. *Research on Chemical Intermediates*, *49*(6), 2455-2493.

Lee, Lawrence Cho-Cheung, & Lo, Kenneth Kam-Wing. (2024). Shining new light on biological systems: Luminescent transition metal complexes for bioimaging and biosensing applications. *Chemical Reviews*, *124*(15), 8825-9014.

Leveraro, Silvia, Dzyhovskyi, Valentyn, Garstka, Kinga, Szebesczyk, Agnieszka, Zobi, Fabio, Bellotti, Denise, Rowińska-Żyrek, Magdalena. (2025). Metal-Induced Amide Deprotonation and Binding Typical for Cu (II), Not Possible for Zn (II) and Fe (II). *Inorganic Chemistry*, *64*(13), 6751-6760.

Malav, Radhika, & Ray, Sriparna. (2025). Recent advances in the synthesis and versatile applications of transition metal complexes featuring Schiff base ligands. *RSC Advances*, *15*(28), 22889-22914.

Marlina, Anita. (2015). *Copper (II), Nickel (II), Cobalt (II), and Iron (II) Complexes of Conjugated Organic Ligands as Potential Dye-Sensitised Solar Cell Materials.* University of Malaya (Malaysia).

Mazen, SA, Elsayed, HM, & Abu-Elsaad, NI. (2021). A comparative study of different concentrations of (Co/Ni/Cu) effects on elastic properties of Li–Mn ferrite employing IR spectroscopy and ultrasonic measurement. *Ceramics International*, *47*(19), 26635-26642.

Mujahid, Muhammad, Trendafilova, Natasha, Rosair, Georgina, Kavanagh, Kevin, Walsh, Maureen, Creaven, Bernadette S, & Georgieva, Ivelina. (2023). Structural and spectroscopic study of new copper (II) and zinc (II) complexes of coumarin oxyacetate ligands and determination of their antimicrobial activity. *Molecules*, *28*(11), 4560.

Mushtaq, Irfan, Ahmad, Maqbool, Saleem, Muhammad, & Ahmed, Adnan. (2024). Pharmaceutical significance of Schiff bases: an overview. *Future Journal of Pharmaceutical Sciences*, *10*(1), 16.

Nagajothi, D, & Maheswari, J. (2021). Synthesis, characterization and antimicrobial activity of Schiff base ligand metal complexes. *GIS Sci. J*, *8*(1), 1314-1326.

Nandini, B, & Selvi, M Amutha. (2025). Metal Complexes with Schiff Bases-A Review of their Antimicrobial Activities. *Current Bioactive Compounds*, *21*(5), E15734072305971.

Ngece, Kwanele, Khwaza, Vuyolwethu, Paca, Athandwa M, & Aderibigbe, Blessing A. (2025). The Antimicrobial Efficacy of Copper Complexes: A Review. *Antibiotics*, *14*(5), 516.

Sankar, Raji, & Sharmila, TM. (2023). Schiff bases-based metallo complexes and their crucial role in the realm of pharmacology. A review. *Results in Chemistry*, *6*, 101179.

Santos, Jayson C dos, Neto, João G, Moreira, Ana BN, da Silva, Luzeli M, Ayala, Alejandro P, Lage, Mateus R, Dos Santos, Adenilson O. (2025). Exploring the Potential of a New Nickel (II): Phenanthroline Complex with L-isoleucine as an Antitumor Agent: Design, Crystal Structure, Spectroscopic Characterization, and Theoretical Insights. *Molecules*, *30*(13), 2873.

Shafie, Alaa, & Ashour, Amal Adnan. (2025). Recent advances in Schiff bases and Cu (II) complexes: Applications in fluorescence imaging and anticancer therapy (2020–2024). *Journal of Inorganic Biochemistry*, 112909.

Sharma, Bharti, Shukla, Sudeep, Rattan, Rohit, Fatima, Musarrat, Goel, Mayurika, Bhat, Mamta, Sharma, Mamta. (2022). Antimicrobial agents based on metal complexes: present situation and future prospects. *International Journal of Biomaterials*, *2022*(1), 6819080.

Soroceanu, Alina, & Bargan, Alexandra. (2022). Advanced and biomedical applications of Schiff-base ligands and their metal complexes: A review. *Crystals*, *12*(10), 1436.

Subitha, S, Kanmoni, V Gnana Glory, Raj, C Isac Sobana, Jona, J, & Vibi, V. (2021). Synthesis, Characterization Study of Schiff base Complexes derived from Ampicillin and 4-Hydroxy-3-methoxy benzaldehyde. *Oriental Journal of Chemistry*, *37*(4), 813.

Takalloo, Fahimeh, Gholizadeh, Ahmad, & Ardyanian, Mahdi. (2024). Crystal structure-physical properties correlation in Ni–Cu–Zn spinel ferrite. *Journal of Materials Science: Materials in Electronics*, *35*(27), 1792.

Uddin, Ekhlass, Sardar, Md Nazmul, Reza, Md Shahin, Hasan, Md Sohag, Talukder, Md Tanvir, Hoque, Md Mahbubul, Asraf, Md Ali. (2025). Emerging pharmaceutically active drugs: synthesis and pharmacology of Schiff base ligands with their metal complexes. *Discover Chemistry*, *2*(1), 153.

Venkatesh, Ganesan, Vennila, Palanisamy, Kaya, Savas, Ahmed, Samia Ben, Sumathi, Paramasivam, Siva, Vadivel, Kamal, Chennapan. (2024). Synthesis and spectroscopic characterization of Schiff base metal complexes, biological activity, and molecular docking studies. *ACS omega*, *9*(7), 8123-8138.

Wasafa, Atheraa Abdul Kadhim, Jaffera, Noor Dia, & Alkuwaityb, Eman Abdul Wahab. (2023). Synthesis, characterization, and studying of (thermal, spectral and physical) properties of new Schiff base monomers and liquid Crystal compounds from Ampicillin. *Synthesis*, *10*, 11.

Waziri, Ibrahim, Yusuf, Tunde L, Zarma, Hauwa A, Oselusi, Samson O, Coetzee, Louis-Charl C, & Adeyinka, Adedapo S. (2023). New palladium (II) complexes from halogen substituted Schiff base ligands: Synthesis, spectroscopic, biological activity, density functional theory, and molecular docking investigations. *Inorganica Chimica Acta*, *552*, 121505.

Yusuf, Tunde L, Oladipo, Segun D, Zamisa, Sizwe, Kumalo, Hezekiel M, Lawal, Isiaka A, Lawal, Monsurat M, & Mabuba, Nonhlangabezo. (2021). Design of new Schiff-Base Copper (II) complexes: Synthesis, crystal structures, DFT study, and binding potency toward cytochrome P450 3A4. *ACS omega*, *6*(21), 13704-13718.

Zalevskaya, OA, & Gur'eva, Ya A. (2021). Recent studies on the antimicrobial activity of copper complexes. *Russian Journal of Coordination Chemistry*, *47*(12), 861-880.

Zavaroni, Alessio, Rigamonti, Luca, Bisceglie, Franco, Carcelli, Mauro, Pelosi, Giorgio, Gentilomi, Giovanna Angela, Bonvicini, Francesca. (2025). Antimicrobial Activity of Copper (II), Nickel (II) and Zinc (II) Complexes with Semicarbazone and Thiosemicarbazone Ligands Derived from Substituted Salicylaldehydes. *Molecules*, *30*(11), 2329.